Realistic Simulated MRI and SPECT Databases
Application to SPECT/MRI Registration Evaluation

Berengere Aubert-Broche[1], Christophe Grova[1], Anthonin Reilhac[1,2], Alan C. Evans[1], and D. Louis Collins[1]

[1] Montreal Neurological Institute, McGill University, Montreal, Canada
[2] CERMEP, Lyon, France

Abstract. This paper describes the construction of simulated SPECT and MRI databases that account for realistic anatomical and functional variability. The data is used as a gold-standard to evaluate four SPECT/MRI similarity-based registration methods.

Simulation realism was accounted for using accurate physical models of data generation and acquisition. MRI and SPECT simulations were generated from three subjects to take into account inter-subject anatomical variability. Functional SPECT data were computed from six functional models of brain perfusion. Previous models of normal perfusion and ictal perfusion observed in Mesial Temporal Lobe Epilepsy (MTLE) were considered to generate functional variability. We studied the impact noise and intensity non-uniformity in MRI simulations and SPECT scatter correction may have on registration accuracy.

We quantified the amount of registration error caused by anatomical and functional variability. Registration involving ictal data was less accurate than registration involving normal data. MR intensity non-uniformity was the main factor decreasing registration accuracy. The proposed simulated database is promising to evaluate many functional neuroimaging methods, involving MRI and SPECT data.

1 Introduction

Digital simulations of imaging modalities provide a way of generating data where a gold-standard is available. They become widely used as evaluation datasets to characterize and optimize the performance of image processing methods. Simulators accurately modelling physical properties of MRI, PET or SPECT data acquisition have been proposed and validated [1, 2, 3]. Realistic simulations are usually obtained from high-resolution human brain data, defining a spatial model of brain anatomy. Such models were based on a single brain [4],[5]. Recently, to take into-account inter-subject anatomical variability for MRI simulations, we built anatomical models from multiple T1, T2 and PD-weighted MRI acquisitions of 20 normal adults (submitted work). Reilhac *et al.* [3] used anatomical MRI from 17 normal adults to simulate PET data.

For realistic simulations of functional data such as SPECT and PET, anatomical models are required to define the attenuation map describing the attenuation properties of head tissues and the activity map representing the 3D spatial dis-

R. Larsen, M. Nielsen, and J. Sporring (Eds.): MICCAI 2006, LNCS 4190, pp. 330–337, 2006.

tribution of the radiotracer. Generating a realistic activity map usually requires measurements on real data, as for instance averaged normal perfusion and averaged ictal perfusion models [6]. Functional variability may be characterized by exploring the structure of covarying areas among functional data issued from homogeneous populations. Principal component analysis [7, 8] and correspondence analysis [9] have proved their ability to characterize normal perfusion and ictal perfusion in patients with MTLE.

In this paper, we propose to adapt anatomical models previously developed to simulate SPECT data. To simulate functional variability, three maps mimicking normal perfusion and three maps mimicking ictal perfusion in MTLE were generated from the main modes of variation of the model proposed in [9]. For each subject and each functional model, MR simulated data were generated with different noise and intensity non-uniformity levels. Simulated SPECT data were reconstructed with and without scatter post-correction. These SPECT and MRI simulated data-sets were used to evaluate four similarity-based registration methods : mutual information (MI), normalized mutual information (NMI), L1 and L2 norm-based correlation ratios (CR).

2 Methods

2.1 MR Simulations

Anatomical Models. The method proposed in [10] was used to create anatomical models from 20 healthy subjects. For each subject, we acquired four T1, T2 and PD-weighted scans. All images were corrected for intensity non-uniformity [11], registered [12] and resampled in the average brain space [13], intensity normalized and averaged to create averaged T1, T2 and PD-weighted volumes for each subject. A fuzzy bayesian classification was used to classify voxel intensities from T1, T2 and PD averaged volumes into grey matter, white matter, cerebro-spinal fluid and fat. Automatically generated mask volumes were employed to separate brain from non-brain structures and to create the following classes of the anatomical model: grey matter, white matter, cerebro-spinal fluid, skull, bone marrow, dura, fat, muscles and skin.

Simulation. Each class of the anatomical model was described by its nuclear magnetic resonance (NMR) relaxation properties. NMR signal intensities were computed for all classes by feeling these NMR parameters into a discrete-event Bloch equation in the MR simulator [1]. The simulator could model noise and RF field inhomogeneity. T1-weighted MRI data were simulated at two levels of noise, i.e., 3% (named 'mri-pn3') and 9% (named 'mri-pn9') standard deviation. A high level of intensity non-uniformity (INU) (60%, named 'mri-rf60') was also simulated from data generated at 3% of noise. Scan parameters were similar to those used during a clinical acquisition (3D spoiled gradient echo (GRE) sequence, $TR = 22ms, TE = 9.2ms, \alpha = 30^o$, 1 mm isotropic voxel size).

2.2 SPECT Simulations

Anatomical Models. For each subject, the grey matter of the MRI anatomical models was subdivided to define the SPECT anatomical models. A digital atlas was first mapped onto the grey matter class, using a non linear registration algorithm to automatically extract the different grey matter regions [14]. These grey matter regions were modified as the anatomical regions usually considered by epilepsy specialists divide the temporal and frontal lobes into their posterior, lateral, mesial and polar areas [6].

Attenuation and Activity Maps. The attenuation map was obtained by assigning an attenuation coefficient μ at the 140 keV energy emission of ^{99m}Tc to each class of the anatomical model. Seven tissue types were considered : connective tissue, water, brain, bone, muscle, fat and blood. The model proposed in [9] was used to generate realistic activity maps accounting for functional variability. 27 SPECT data from healthy subjects and 10 ictal SPECT from patients with MTLE were first spatially and intensity normalized into an average brain space. The digital atlas described above was then used to perform Volume of Interest (VOI)-based measurements on each SPECT data. The structure of covariance among these VOI measurements over all SPECT data was measured using correspondence analysis. Five principal components accounting for 67.5% of total variance were selected to model normal perfusion. Two principal components accounting for 69.2% of total variance were considered for ictal perfusion. Three healthy subjects and three patients with MTLE were first randomly selected. Six activity maps mimicking normal perfusion (N1, N2, N3) and ictal perfusion in MTLE (I1, I2, I3) were then generated by projecting the VOI measurements of each subject on the corresponding selected principal components. This projection aims at removing measurement noise in the data in order to account only for the main modes of perfusion variability.

Simulation and Reconstruction. Using attenuation and activity maps, Monte Carlo simulations were performed using the SimSET[1] simulator [15]. Projections were simulated using a 20% energy window centred on 140 keV (126-154 keV) and a Compton window (111-125 keV). Attenuation and Compton scatter were modelled through Monte Carlo methods. The collimator and gamma camera responses were modelled through analytical models. To assess the impact of scatter correction on registration accuracy, Jaszczak scatter correction was applied by subtracting the simulated projections of the Compton window from the simulated projections of the 20 % energy window centred on 140 keV. All projections were reconstructed by filtered backprojection using a ramp filter (Nyquist frequency cutoff). The reconstructed data (4.51 mm isotropic voxel size) were post-filtered with a 3D Gaussian filtering (FWHM = 8mm).

[1] Simulation of Emission Tomography (SimSET) package, *http : //depts.washington.edu/ simset/html/simset_main.html*

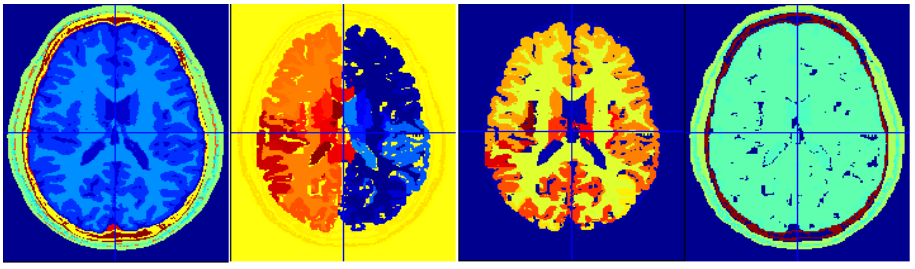

(A) (B) (C) (D)

Fig. 1. For the first subject,(A) anatomical model used for MRI simulation, (B) grey matter subdivided-model used for SPECT simulation, (C) an activity map modelling normal perfusion and (D) an attenuation map obtained from this model

2.3 SPECT/MRI Registration Evaluation

Registration Methods. These simulated data were used to evaluate four statistical similarity-based SPECT/MRI registration methods: mutual information (MI), normalized mutual information (NMI), L1 and L2 norm-based correlation ratios (CRL1 and CRL2). Each registration method was implemented as proposed by [16].

Evaluation. We studied the impact anatomical and functional variabilities generated by the proposed simulated data have on registration performance. For each subject and for each functional model, we computed registrations between three simulated MRI data (two with different noise levels and one with INU) and two SPECT reconstructions (with and without photon scatter correction). Table 1 summarize the different simulations contexts. For each subject, the three simulated MR volumes are registered to twelve SPECT volumes using four different similarity measures.

Since the simulated SPECT data was perfectly aligned with simulated MRI data by construction, we applied a known geometrical transformation to the simulated MRI data to generate mis-aligned data. For each simulation context, 20 known transformations were generated by randomly sampling a six parameters vector using a Gaussian distribution (mean = 0, standard deviation = 10 mm or ^{o}). Comparing the known geometrical transformation to the resulting computed transformation, local target registration errors (TRE) were estimated on 200 points uniformly distributed within the brain of each subject. The root mean square value (RMS) of the local errors distribution was estimated to characterize the spatial distribution of TRE within the brain.

3 Results

3.1 MRI and SPECT Simulations

For the first subject, Fig. 1 shows transverse slices of the anatomical model used for MRI simulation, the grey matter subdivided-model used for SPECT simula-

Table 1. Simulation contexts explored by SPECT/MRI registration evaluation

Anatomical model	Functional model	MRI data quality	SPECT data quality	Registration methods
3 subjects	- 3 normal models - 3 ictal models	- 3% noise - 9% noise - 3% noise and INU	- scatter correction - no scatter correction	- CRL1 - CRL2 - MI - NMI

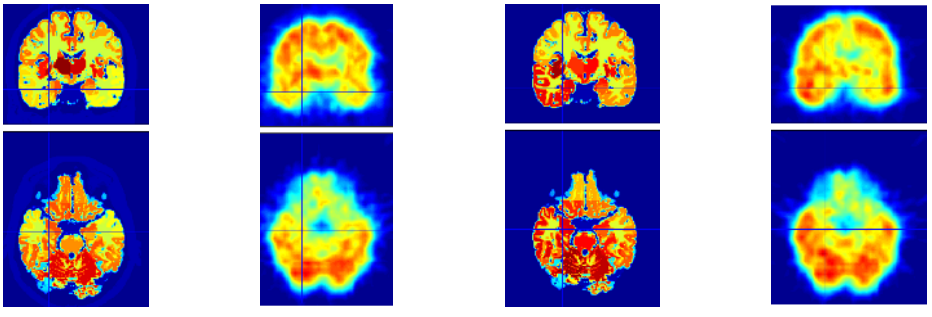

(A) (B)

Fig. 2. For the first subject, activity maps and simulated spect (A) with normal perfusion N1 and (B) with ictal perfusion I1

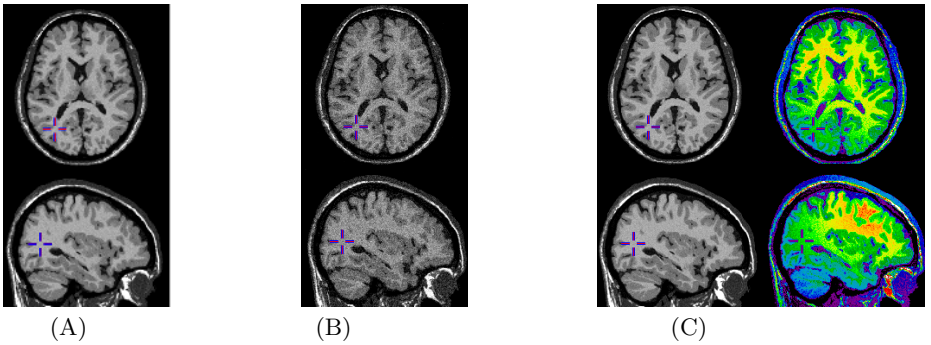

(A) (B) (C)

Fig. 3. For the first subject, simulated MRI (A) with 3% noise, (B) with 9% noise and (C) with 3% noise and 60% intensity non-uniformity

tion, a normal activity map and an attenuation map obtained from this model. To illustrate functional variability, two activity maps and resulting simulated SPECT are shown Fig. 2. Fig. 3 shows MRI simulated data of the same subject for different noise levels and INU.

3.2 Registration Evaluation

Distribution of registration RMS errors (in mm) are summarized using boxplot distributions in Fig. 4. Whereas increasing levels of noise in MRI data had slight

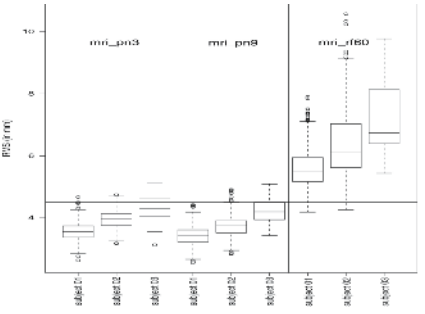

(a) Effect of anatomical variability (3 subjects)

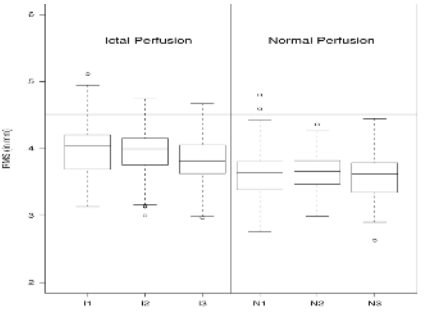

(b) Effect of functional variability (6 functional models: ictal perfusion I1, I2 and I3 and normal perfusion N1, N2 and N3 with mri-pn3)

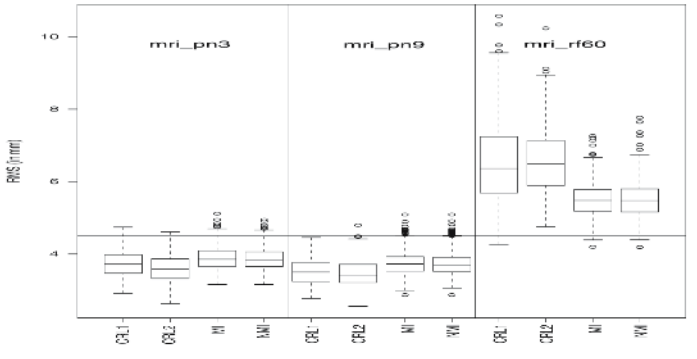

(c) Effect of the registration method

Fig. 4. Distributions of SPECT/MRI registration errors (RMS in mm) for different MRI data "quality": 3% noise (mri-pn3), 9% noise (mri-pn9) and 3% noise with intensity non-uniformity (mri-rf60). Results obtained for all parameters omitted in the captions were pooled together in the boxplot representations. Horizontal line indicates SPECT voxel size at 4.51 mm

impact on registration accuracy, generating high intensity non-uniformity level on MRI data (60%) clearly decreased registration accuracy (Fig. 4(a) and (c)). We showed also an impact of anatomical variability on registration performance (Fig. 4(a)). Analysis of variance confirms a significant effect of the subjects and MRI data quality on registration accuracy (F=3834, R^2_{adjust}=0.82, p <0.001). We found no effect of scatter post-correction of SPECT data on registration accuracy (results not shown).

We observed a significant effect of the clinical context (ictal vs normal perfusion) on registration accuracy (analysis of variance, F=232.5, R^2_{adjust}=0.21, p <0.001). Registrations involving normal SPECT simulations were significantly

more accurate than registrations involving ictal data (Fig. 4(b)). Although small variations due to functional variability were observed within each perfusion group (ictal or normal)(Fig. 4(b)), main trends concerning the loss of registration accuracy in pathological condition were still present. In presence of INU, MI and NMI based registrations were slightly more accurate than CRL1 and CRL2 methods (Fig. 4(c)). The opposite situation was observed when considering MRI simulations without INU.

4 Discussion and Conclusion

The simulation database computed for this study enables one to take into account both anatomical variability, using anatomical models from three subjects, and functional variability, considering six functional models (ictal and normal). Using fully controlled simulated data, the impact of many data quality parameters could be studied, such as noise and INU levels in MRI data, or SPECT data scatter correction. Accounting for anatomical and functional variability in simulated databases is essential for validation of statistical analysis methods, as for instance epileptogenic focus detection methods or inter-subject group analysis methods. We plan to make these images publicly available on the internet for comparison of different methods.

Assessing the realism of the simulations is an important and difficult issue. All simulated data rely on techniques reproducing accurately the physics of data generation and acquisition [1, 2]. To evaluate the realism of simulated data, previous studies reported comparison between mean intensities measurements between real and simulated SPECT data [6]. From the 20 subjects acquired for this project, voxel-based group comparison between simulated and real T1-weighted data confirmed the realism of MRI simulations (submitted work). We plan to use a similar approach to assess the realism of our simulated SPECT data. Note that the realism of the method used to characterize perfusion variability should also be assessed, using a leaving-one-out evaluation procedure for instance [7].

The SPECT/MRI registrations evaluated in this study illustrate an important application of SPECT and MRI simulated databases. We quantified the amount of registration error variability caused by simulated anatomical and functional variability. Our results were in agreement with [16], showing that registration of pathological data was less accurate than registration of normal data, due to an increase in intensity dissimilarity between data. The major result was the important decrease of registration accuracy due to a high intensity non-uniformity on MRI data, which has never been studied before in the context of SPECT/MRI registration. However, the effect of MRI intensity non-uniformity was demonstrated for T1-T2 NMI registration [17]. The proposed framework is ideal to quantify the impact of several INU levels on registration accuracy or to quantify if correction methods [11] may improve SPECT/MRI registration accuracy.

We are currently working on the extension of this simulated database. We plan to use the 20 anatomical models already available, as well as more perfusion models, using random sampling of activity values within the main modes of variation.

References

1. R. Kwan, A.C. Evans, and G.B. Pike. MRI simulation-based evaluation of image-processing and classification methods. *IEEE Trans Med Imaging*, 18(11):1085–1097, 1999.
2. I. Buvat and I. Castiglioni. Monte carlo simulations in SPET and PET. *Quarterly J. Nucl. Med.*, 46:48–59, 2002.
3. A. Reilhac, G. Batan, C. Michel *et al.* PET-SORTEO: validation and development of database of simulated PET volumes. *IEEE Trans Nucl Sci.*, 52(5):1321–1328, 2005.
4. IG Zubal, CR Harrell, EO Smith *et al.* Computerized three-dimensional segmented human anatomy. *Med Phys*, 21(2):299–302, 1994.
5. D.L. Collins, A.P. Zijdenbos, V. Kollokian *et al.* Design and Construction of a Realistic Digital Brain Phantom. *IEEE Trans Med Imaging*, 17(3):463–468, June 1998.
6. C. Grova, P. Jannin, A. Biraben *et al.* A methodology for generating normal and pathological brain perfusion spect images for evaluation of mri/spect fusion methods: application in epilepsy. *Phys Med Biol*, 48(24):4023–4043, 2003.
7. T. Vik, F. Heitz, I. Namer, and J-P. Armspach. On the modeling, construction, and evaluation of a probabilistic atlas of brain perfusion. *Neuroimage*, 24(4):1088–1098, 2005.
8. BJ Weder, K Schindler, TJ Loher *et al.* Brain areas involved in medial temporal lobe seizures: A principal component analysis of ictal spect data. *Human Brain Mapp*, 2005.
9. C. Grova, P. Jannin, I. Buvat *et al.* From anatomic standardization analysis of perfusion spect data to perfusion pattern modeling: evidence of functional networks in healthy subjects and temporal lobe epilepsy patients. *Acad Radiol*, 12(5):554–565, 2005.
10. B Aubert-Broche, DL Collins, and AC Evans. A new improved version of the realistic digital brain phantom. *Neuroimage*, 2006. in press.
11. J.G. Sled, A.P. Zijdenbos, and A. Evans. A Nonparametric Method for Automatic Correction of Intensity Nonuniformity in MRI Data. *IEEE Trans Med Imaging*, 17(1):87–97, February 1998.
12. DL Collins, P Neelin, TM Peters, and AC Evans. Automatic 3D intersubject registration of MR volumetric data in standardized Talairach space. *J Comput Assist Tomogr*, 18(2):192–205, Mar-Apr 1994.
13. A.C. Evans, D.L. Collins, S.R. Mills *et al.* 3D statistical neuroanatomical models from 305 MRI volumes. In *IEEE Nuclear Science Symposium and Medical Imaging Conference*, pages 1813–1817, San Francisco, USA, October 1993.
14. DL Collins, AP Zijdenbos, WFC Barre, and Evans AC. ANIMAL+INSECT: Improved cortical structure segmentation. In *Proc. of the Annual Symposium on IPMI*, pages 210–223, 1999.
15. R.L. Harrison, S.D. Vannoy, D.R. Haynor *et al.* Preliminary experience with the photon history generator module of a public-domain simulation system for emission tomography. *IEEE Nucl Sci. Symposium*, 2:1154–1158, 1993.
16. C Grova, P Jannin, I Buvat *et al.* Evaluation of registration of ictal SPECT/MRI data using statistical similarity methods. In *MICCAI (1)*, pages 687–695, Saint-Malo, France, September 2004.
17. ZF Knops, JB Maintz, MA Viergever, and JP Pluim. Normalized mutual information based registration using k-means clustering and shading correction. *Med Image Anal.*, 2005.